

High performance silicon carbide avalanche-p-i-n ultraviolet photodiode with dual operation models

Mingkun Zhang, Kang L. Wang, Hexin Jiang, Rongdun Hong[✉] and Zhengyun Wu

Silicon carbide-based quasi-separated-absorption-multiplication ultraviolet avalanche photodiode (APD) with a small-area multiplication region and a large-area absorption region, which comprises of a p^+nn^- junction encircled by a p^+n^- junction, is proposed, and its optoelectronic performance is modelled. The modelling results show a 4H-SiC APD with high performance can be achieved. Moreover, when operated at a low reverse bias (e.g. 5.0 V), the photodiode has almost the same optoelectronic characteristics as the 4H-SiC p-i-n photodiode. It is noted that the device has benefited advantages of both conventional separate absorption and multiplication APD and p-i-n photodiode in the wavelength range of ultraviolet detection, which enable the dual operation models of the device.

Introduction: The avalanche photodiodes (APDs) are dominating in the research field of the weak signal and single photon ultraviolet (UV) detection for its carrier's avalanche multiplication process. Moreover, the separate absorption and multiplication (SAM) APDs have the advantages of providing single carrier injection, high quantum efficiency, low multiplication noise and low operating voltage. To obtain a high detectivity, SAM APDs with large area should be employed, as the detectivity is proportional to the square root of the sensitive area [1]. However, there is a higher probability of a device containing defects as it gets larger and these causing high dark current, instability and premature breakdown [2]. One approach to circumventing the 'defect problem' is to fabricate arrays of small diameter APDs. The motivation for this approach is that the bad array elements can be disconnected. While this will reduce the photosensitive area of the array, a localised defect will not be catastrophic as it would in a single large-area detector [3]. This Letter proposes a 4H-SiC SAM photodiode with a small multiplication area and a large-area absorption region, which is another approach to circumvent the 'defect problem'. Moreover, the 4H-SiC photodiode has merits of both SAM APD and p-i-n photodiode, and is named as a SAM avalanche-p-i-n (APIN) photodiode.

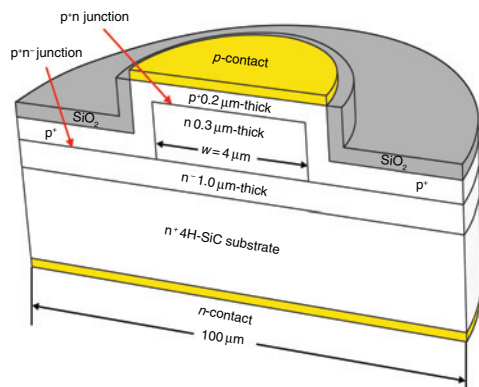


Fig. 1 Structures of 3D structure of 4H-SiC APIN photodiode

Modelling results and discussion: The three-dimensional (3D) device modelling was accomplished by using the ATLAS software package from SILVACO. Moreover, the governing physical models specified in the ALTAS program was based on Cha's report [4]. Fig. 1 shows the typical 3D device structure of the 4H-SiC APIN photodiode, which features a large bulk absorption region underneath a small multiplication region, built on a 100.0 μm diameter n^+ -type substrate. On the substrate, a 1.0 μm-thick n^- -type layer is designed as the absorption region and a 0.3 μm-thick n^- -type layer is designed onto the surface centre of the n^- -type to provide a multiplication region. The diameters of the n^- -type layer and the n^- -type layer are 100.0 and 4.0 μm. Then, the surface of the device is covered by a 0.2 μm-thick p^+ -type capping layer, followed by a 0.3 μm-thick SiO_2 passivation layer onto the step of the mesa structure. The doping concentrations for p^+ , n , n^- and n^+ layers are 2.0×10^{19} , 7.0×10^{17} , 1.0×10^{15} and $1.0 \times 10^{19} \text{ cm}^{-3}$, respectively. The conventional 4H-SiC SAM ($p^+nn^-n^+$) APD and p-i-n

($p^+n^-n^+$) photodiode were also modelled. The doping concentration and the thickness for each layer of the APD and p-i-n are the same as those of the APIN photodiode. Moreover, the sensitive areas of all photodiodes are the same.

Fig. 2 illustrates the reverse dark current-voltage characteristics and the photocurrent-voltage characteristics of 4H-SiC SAM APD, APIN and p-i-n photodiodes. The wavelength and the power density (I) of the UV irradiation are 270 nm and $4.0 \times 10^{-3} \text{ W/cm}^2$, respectively. The results illustrate the avalanche breakdown voltage (V_{br}), corresponding to an avalanche gain M of 1000, of the 4H-SiC APIN photodiode is about 107.5 V, which is almost as small as that ($\sim 100.3 \text{ V}$) of the conventional 4H-SiC SAM APD and much smaller than that ($\sim 247.1 \text{ V}$) of the p-i-n photodiode. Here, the avalanche gain M is calculated conventionally by the following equation:

$$M = \frac{I_{\text{photo-M}} - I_{\text{dark-M}}}{I_{\text{photo}} - I_{\text{dark}}} \quad (1)$$

where $I_{\text{photo-M}}$ and $I_{\text{dark-M}}$ are the multiplied photocurrent and dark current, respectively, while I_{photo} and I_{dark} are the un-multiplied photocurrent and dark current.

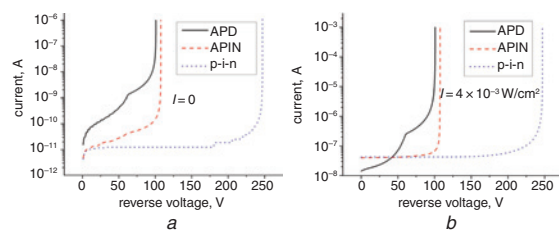


Fig. 2 Reverse current-voltage characteristics of 4H-SiC APD, APIN and p-i-n photodiodes

- a Without UV irradiation
- b With UV irradiation

The low V_{br} of APIN photodiode is because the avalanche multiplication initiates first in the p^+n^- junction, in which the breakdown electric field intensity is the same as the conventional SAM APD, for the same doping concentration of the n layers for both photodiodes. However, due to the interaction between the electric fields of p^+n^- junction and p^+n junction, the V_{br} of the APIN photodiode would be slightly larger than that of the conventional APD. Fig. 2a also illustrates that, compared with APD, the APIN photodiode possesses a relatively low dark current, which is attributed to the small area of the multiplication region (n layer).

In Fig. 2b, when the reverse voltage is below 42.0 V, the photocurrent of the APD is smaller than the photocurrents of the APIN and p-i-n photodiodes. While the reverse voltage is higher than 42.0 V, the photocurrent of the APD becomes larger than those of the APIN and p-i-n photodiodes. The low photocurrent of the APD at low reverse voltage is due to the non-punch-through depletion layer, as shown in Fig. 3a, which leads to a low quantum efficiency. The photocurrent of APD will increase obviously with the reverse voltage due to the depletion layer broadened with the increase of the reverse voltage. Moreover, the high photocurrents of the APIN and p-i-n photodiodes are attributed to the punch-through depletion layer (Figs. 3b and c). Moreover, before the avalanche breakdown, the photocurrents of the APIN and p-i-n photodiodes are almost identical and scarcely changed, which is attributed to the non-carrier-multiplication and the punch-through of the depletion layer for both devices. On the other hand, with the increase of reverse voltage from 42.0 V, the carrier multiplication will initiate first in the APD for the high electric field intensity near the p^+n^- junction caused by the high doping level of the n layer [5], which results in a larger photocurrent of APD.

The spectral responsivities of 4H-SiC p-i-n and APIN photodiodes biased at 5 V are illustrated in Fig. 4a. It is noted the responsivity curves for both devices are almost identical, which indicates that the 4H-SiC APIN photodiode has the same characteristics as 4H-SiC p-i-n photodiode at 5 V in the area of UV detection. The resemblance of the responsivity curves of the 4H-SiC p-i-n and APIN photodiodes is because, as biased at a low reverse voltage, the depletion layers of both devices punch through to the substrates (illustrated in Fig. 3),

which ensure the maximum photon absorption and separation of photo-generated carriers.

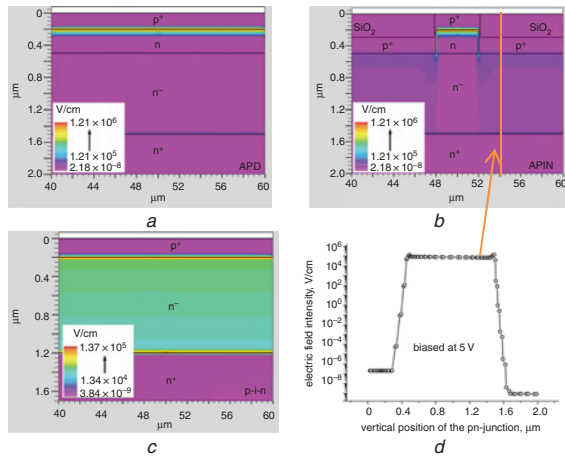


Fig. 3 Electric field density distributions of photodiodes biased at 5 V
 a For 4H-SiC APD
 b For 4H-SiC APIN photodiode
 c For 4H-SiC p-i-n photodiode
 d For 4H-SiC APIN photodiode at vertical position of pn^- junction

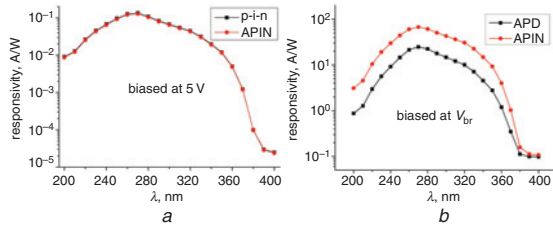


Fig. 4 Responsivities of devices
 a For 4H-SiC p-i-n and APIN photodiodes biased at 5 V
 b For 4H-SiC APD and APIN photodiodes biased at V_{br}

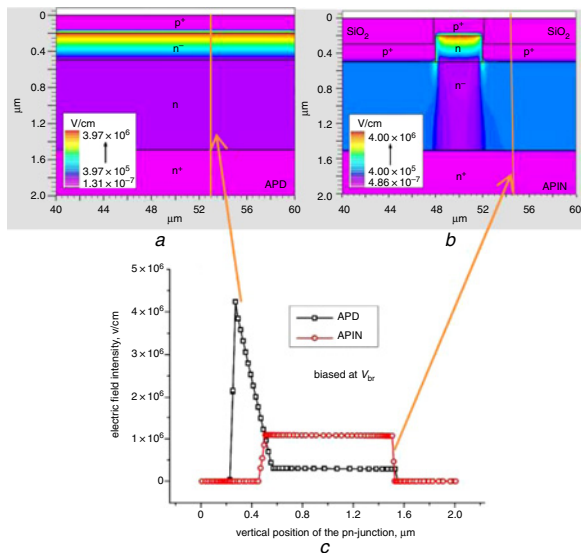


Fig. 5 Electric field density distributions biased at V_{br}
 a For 4H-SiC APD
 b For 4H-SiC APIN photodiode
 c For APD and APIN at vertical position of pn^- junction

The spectral responsivities of 4H-SiC APD and APIN photodiodes biased at V_{br} are illustrated in Fig. 4b. It is noted that, in the wavelength range from 200 to 400 nm, the 4H-SiC APIN photodiode has obviously higher responsivity than the 4H-SiC APD. Compared with the APD, the APIN structure of a large bulk absorption region underneath a small multiplication region (as shown in Figs. 3a and b) can avoid the high photon-generated carrier recombination rate caused by the high doping level of n layer. Therefore, for APIN photodiode, more photon-generated carriers will be collected to turn into the photocurrent. Moreover, according to Fig. 5, if the electric field intensity in the absorption area of the APIN photodiode is greater than that of the APD, it can more effectively separate the photon-generated carriers. Therefore, more photon-generated carriers could be devoted to the multiplication process of the APIN photodiode at the avalanche V_{br} , leading to the higher responsivity of the APIN photodiode than that of the APD. Therefore, compared with the APD, 4H-SiC APIN photodiode would have a higher responsivity.

Conclusions: This Letter proposes a 4H-SiC photodiode of quasi-SAM structure featuring a small-area multiplication region and a large bulk absorption region, which ensure the low dark current, low breakdown voltage and abundant absorption of the photons. When biased at reverse V_{br} , the 4H-SiC APIN photodiode with high performance can be achieved. Moreover, as operated at low reverse bias, the 4H-SiC APIN photodiode has almost same characteristics as p-i-n photodiode. Therefore, the 4H-SiC APIN photodiode can be operated at dual models.

Acknowledgments: This work was supported by the National Natural Science Foundation of China (61307047) and the Fundamental Research Funds for the Central Universities (20720160123).

© The Institution of Engineering and Technology 2016
 Submitted: 6 June 2016 E-first: 2 August 2016
 doi: 10.1049/el.2016.2025

One or more of the Figures in this Letter are available in colour online.

Mingkun Zhang, Hexin Jiang, Rongdun Hong and Zhengyun Wu (*Physics and Mechanical and Electrical Engineering School, Xiamen University, Xiamen 361005, Fujian, People's Republic of China*)

✉ E-mail: rdhong@xmu.edu.cn

Kang L. Wang (*Electrical Engineering Department, University of California, Los Angeles, CA 90095, USA*)

References

- Bai, X., Liu, H.D., McIntosh, D.C., and Campbell, J.C.: 'High-detectivity and high-single-photon-detection-efficiency 4H-SiC avalanche photodiodes', *J. Quantum Electron.*, 2009, **45**, (3), pp. 300–303, doi: 10.1109/JQE.2009.2013093
- Vert, A., Soloviev, S., and Sandvik, P.: 'SiC avalanche photodiodes and photomultipliers for ultraviolet and solar-blind light detection', *Phys. Status Solidi A*, 2009, **206**, (10), 2468–2477, doi: 10.1002/pssa.200925118
- Liu, H.D., Zheng, X., Zhou, Q., Bai, X., McIntosh, D.C., and Campbell, J.C.: 'Double mesa sidewall silicon carbide avalanche photodiode', *J. Quantum Electron.*, 2009, **45**, (12), 1524–1528, doi: 10.1109/JQE.2009.2022046
- Cha, H.Y., and Sandvik, P.M.: 'Electrical and optical modeling of 4H-SiC avalanche photodiodes', *Jpn. J. Appl. Phys.*, 2008, **47**, (7), 5423–5425, doi: 10.1143/JJAP.47.5423
- Sze, S.M., and Ng, K.K.: 'Physics of semiconductor devices' (Wiley, Hoboken, New Jersey, USA, 2007, 3rd edn.)